Molecular Interactions of 3′,5′-Cyclic Purine Analogues with the Binding Site of Retinal Rod Ion Channels†

Sean-Patrick Scott‡ and Jacqueline C. Tanaka*,§

Department of Biochemistry and Biophysics, School of Medicine, and Department of Pathology, School of Dental Medicine, University of Pennsylvania, Philadelphia, Pennsylvania 19104

Received August 29, 1994; Revised Manuscript Received December 15, 1994⊗

ABSTRACT: Photoreceptor outer segments transduce information about incoming light levels through a class of ion channels that respond directly to changes in cytosolic 3′,5′-cyclic guanosine monophosphate levels. A series of 3′,5′-cyclic purine analogues with alterations at N1, C2, C6, or C8 positions was used to examine molecular interactions between the nucleotide and the channel. The maximal current activated by C2-altered analogues in excised membrane patches was less than the current activated by cGMP, and the $K_{0.5}$, the concentration which activates 50% of the current in a patch, was increased. Nonpolar C8-substituted cAMP analogues activated more current than the parent cAMP with lower $K_{0.5}$ values. This was in contrast to 8-amino-cAMP, which exhibited greatly reduced activity. The rank order of activity, based on $K_{0.5}$ values, for C8-cAMP substituents was as follows: 8-azido- > 8-methylamino- > 8-benzylamino- > cAMP > 8-bromo- > 8-hydroxy- ≫ 8-amino-cAMP. 1,N^6-Etheno-cAMP and N^6-monobutyryl-cAMP activated a small fraction of the total possible current with high $K_{0.5}$ values. Other analogues with alterations at N1 or C6 positions including N^1-oxide-cAMP, 2-aminopurine riboside 3′,5′-monophosphate, and N^6-monosuccinyl-cAMP do not bind to the channel, suggesting that interactions with the channel in this region are essential for binding. In order to help interpret the changes in maximal current and $K_{0.5}$ values compared to cGMP, molecular models of the active analogues were constructed and then docked into a molecular model of the cyclic nucleotide binding site of the retinal channel. This model, proposed by Kumar and Weber [(1992) *Biochemistry 31*, 4643−4649], was based on the crystal structure of cAMP bound to catabolite activator protein. Our modeling showed that the analogues were sterically accommodated within the binding site. No hydrogen bonds were predicted between the purine rings of cAMP and the pocket; however, Phe 533 on the β5 strand was predicted to form weak electrostatic interactions with C6 substituents on both cAMP and cGMP. The importance of contacts in this region of the binding pocket is further emphasized by the inactive analogues, all of which are altered at N1 or C6.

In the absence of experimentally determined structures to atomic resolution for ion channel proteins, channel agonists and antagonists have been used successfully to derive details of molecular architecture (Hille, 1992). One important class of ion channels found on sensory neurons transduces information detected by the neuron into an electrical signal. In retinal rods, incoming photons are detected by rhodopsin, and information about the light flux is relayed through a biochemical cascade which terminates in changes of cytosolic 3′,5′-cyclic GMP levels (Kaupp, 1991; Yau & Baylor, 1989). The retinal rod ion channels responding directly to changes in cGMP levels display a ~50-fold preference for cGMP[1] over cAMP (Tanaka et al., 1989). Since cAMP and cGMP differ chemically only at the C2 and C6 positions on the purine, strategic contacts at these positions may mediate communication from the binding site to other domains of the channel protein and to other subunits in this multimeric assembly (Kaupp et al., 1989). To examine the interactions between the binding site and the purine, we assayed the ability of a series of cyclic nucleotide analogues to activate current in salamander photoreceptor excised patches and interpreted the results with a three-dimensional model of the nucleotide binding site. The analogues had chemical alterations at positions N1, C2, C6, or C8 on the purine. Our electrophysiological experiments showed that (a) alterations at each of these positions on the purine were tolerated in contrast to previous studies, which showed that most alterations of the ribofuranose result in the loss of activity (Tanaka et al., 1989; Zimmerman et al., 1985); (b) certain alterations at C8, particularly the addition of hydrophobic substituents, can decrease the $K_{0.5}$ for current activation, suggesting that the ligands bind more tightly to the channel; (c) all alterations at C2 result in an increased $K_{0.5}$ and a decrease in the maximal current activated compared to that activated by cGMP; and (d) alterations at N1 and C6 form crucial contacts since three analogues modified at these positions showed no binding.

† This work was supported by NIH Grant EY06640. A preliminary report of this work was presented at the Biophysical Society Meeting (Scott et al., 1994).

* Correspondence should be addressed to this author: Phone: 215-898-4769; FAX: 215-898-5243; e-mail address: tanaka@athens.dental.upenn.edu.

‡ School of Medicine.

§ School of Dental Medicine.

⊗ Abstract published in *Advance ACS Abstracts,* February 1, 1995.

[1] Abbreviations: cIMP, cyclic inosine 3′,5′-monophosphate; 2-amino-cPMP, 2-aminopurine riboside 3′,5′-monophosphate; 8-fluorescein-cGMP, cyclic 8-[[(fluorescein-5-ylcarbamoyl)methyl]thio]guanosine 3′,5′-monophosphate; 6-thio-cGMP, 2-amino-6-mercaptopurine riboside 3′,5′-monophosphate; cGMP, 3′,5′-cyclic guanosine monophosphate; cAMP, 3′,5′-cyclic adenosine 5′-monophosphate.

0006-2960/95/0434-2338$09.00/0

The cGMP-activated retinal channel is presently the only ion channel for which a three-dimensional model of the agonist binding domain is available. The model (Kumar & Weber, 1992) was based on the experimentally determined structure of the catabolite gene activator protein (CAP) from *Escherichia coli* (Weber & Steitz, 1987; McKay et al., 1982). In this paper, we constructed molecular models of the analogues and docked them into the model of the retinal ion channel binding site. Following energy minimization, all active ligands were sterically accommodated within the binding site. No direct interactions were predicted between the purine rings of cAMP and the binding site whereas the Kumar and Weber model with cGMP in the binding site predicted a hydrogen bond between the C2 amino of cGMP and the hydroxyl on the side chain of Thr 560. Our modeling predicts weak electrostatic interactions between the substituents located at C6 for both cAMP and cGMP and the phenyl ring of Phe 533 located on β strand 5 of an 8-stranded β-barrel structure. The inactive analogues are altered in such a way that the interactions with Phe 533 would be disrupted, offering additional support for the idea that interactions between β5 and the purine rings are essential for binding.

MATERIALS AND METHODS

Materials. All nucleotides were purchased from Sigma Chemical Co. *Ambystoma tigrinum* were supplied by Charles Sullivan Co., Nashville, TN.

Electrophysiology. The retinas of dark-adapted tiger salamanders, *Ambystoma tigrinum*, were dissected under red light as previously described for frog (Furman & Tanaka, 1989). The experimental solutions used in both the patch electrodes and bath contained 120 mM NaCl, 5 mM HEPES, pH 7.4, and 2 mM of both EDTA(Na) and EGTA(Na). Photoreceptors were layered onto the floor of the experimental chamber, and currents were recorded from excised inside-out patches as previously described (Furman & Tanaka, 1990) using Corning 0010 glass patch pipets. All experiments were done in room light at 19−22 °C. The patch clamp amplifier output (Dagan 8900) was low-pass filtered at 1 kHz before digitization by an IBM AT (5 kHz, 12-bit A/D). Current−voltage relations were measured by applying a linear voltage ramp (260 mV/s) from −90 to +90 mV (Tanaka et al., 1989). Nucleotide-activated currents were measured by positioning the patch pipet in the inflow stream to the chamber manually selected from a set of solutions. Maximal current was measured in each patch by exposing the cytosolic face of the patch to 200 μM cGMP before and after applying a series of analogue test solutions. Current−voltage (IV) relations were calculated by subtracting the leak current, measured in the absence of any nucleotide, from the nucleotide-activated current.

Fitting of Dose−Response Data. Currents measured at each analogue concentration were normalized against the current activated by 200 μM cGMP at that voltage. The current activation is weakly voltage dependent with ~400 mV/*e*-fold shift of the $K_{0.5}$ values (Tanaka et al., 1989). Usually the voltage chosen for analysis was +80 mV, but in some cases the cGMP currents were saturated at these potentials, and lower potentials were used for the fitting. Where relevant, the voltage is stated in the results. The normalized currents were then plotted as a function of the test concentration, and the data were fitted to the equation:

$$\text{fraction of current} = I_{nor}/[1 + (K_{0.5}/L)^{N_h}] \quad (1)$$

with a nonlinear Levenberg−Marquardt fitting routine in TableCurve (Jandel Scientific, Corte Madera, CA) where I_{nor} is the normalized maximal response, L is the ligand concentration, $K_{0.5}$ is the concentration at 50% of the I_{nor}, and N_h is the cooperativity index.

Molecular Models of cGMP and cAMP Analogues. Molecular models of cGMP and cAMP analogues were constructed using the molecular modeling package Builder in InsightII (Biosym Technologies, San Diego, CA) on a Silicon Graphics 4D/35 IRIS computer. The coordinates for the syn form of cGMP in the model for the cGMP binding domain of the retinal rod channel (Kumar & Weber, 1992) were used as a template for constructing the other analogues. All analogues were energy minimized using Discover (InsightII) with 1000 iterations of the Newton−Raphson minimization algorithm cutoff at an RMS difference of <0.01 kcal/mol. The nonbonded terms of the empirical energy function used a Lennard−Jones potential energy function for a 6−12 van der Waals potential and a Coulombic potential with a 5-Å cutoff. As an independent check of the accuracy of ligand modeling, cGMP was constructed from the fragment library using Builder. This model was indistinguishable from the cGMP in the retinal binding site model and from the structure determined by X-ray crystallography (Druyan et al., 1976).

Minimization of the Model with Other Ligands in the Binding Pocket. Coordinates for the molecular model of the cGMP binding domain of the bovine retinal ion channel were provided by Kumar and Weber (1992). The minimization procedure constrained all backbone atoms to the original coordinates and the side chains beyond 5 Å from the ligand with charges fixed at pH 7.2. The energy minimization was carried out with a conjugate gradient algorithm in Discover using consistent valence force field (CVFF) until the RMS difference was less than 0.1 kcal/mol. In addition to predicting steric interactions and hydrogen bonds between the ligands and the binding site, InsightII can also predict the energy of interaction. Overall, we found that these predictions did not correlate with the rank order of apparent binding affinities based on $K_{0.5}$ values, and no further effort was made to interpret these energies.

RESULTS

Activity Measurements of 3′,5′-Cyclic Purine Analogues

3′,5′-Cyclic purine analogues were tested for their ability to activate current in excised membrane patches from salamander photoreceptors. The maximal response of each patch was determined by recording the current in the presence of 200 μM cGMP.

Alterations at the C2 Position. Dose−response relations for cGMP, cAMP, and N^2-monobutyryl-cGMP are shown for representative patches in Figure 1. The dose−response relation for cGMP was fitted with a $K_{0.5}$ value of 15.9 μM and an index of cooperativity, N_h, of 1.9. This N_h value is consistent with the idea that the channel is formed from multiple subunits, each with a single cGMP binding site (Kaupp et al., 1989). Sequence homology with the Shaker K channel, known to be a tetramer (MacKinnon, 1991), suggests that the retinal channel might also be tetrameric;

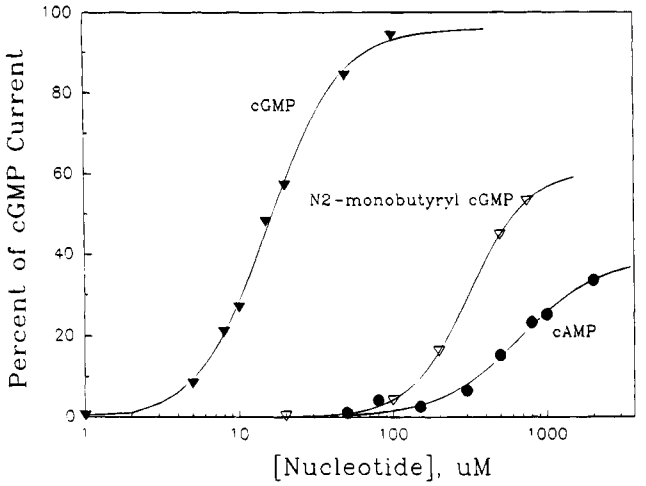

FIGURE 1: Normalized dose–response relations for cGMP, N^2-monobutyryl cGMP, and cAMP. Current vs voltage relations (IV) were measured in excised inside/out patches from salamander photoreceptors in response to bath perfusion with various concentrations of nucleotide analogues as described in the Methods. The $K_{0.5}$ values were 15.9, 312, and 673 μM for cGMP, N^2-monobutyryl cGMP, and cAMP, respectively, with N_h values of 1.9, 2.2, and 1.7. The maximal current in these patches was 61% for N^2-monobutyryl cGMP and 39% for cAMP. The potentials used to determine the fitting for N^2-monobutyryl cGMP and cAMP were +60 and +70 mV, respectively.

Table 1: cGMP Analogues[a]

derivative	2	6	8	$K_{0.5}$
cGMP	NH_2	O	H	13.7 μM(3)
N^2-monobutyryl-cGMP	N2-CO-C_3H_7	O	H	313 μM(1)
cAMP	H	NH_2	H	617 μM(3)
N^6-monobutyryl-cAMP	H	N6-CO-C_3H_7	H	ND[b]
N^6-monosuccinyl-cAMP	H	N6-CO-C_2H_4-CO_2^-	H	ND
2-amino-cPMP	NH_2	H	H	ND
N^1-oxide-cAMP	H	NH_2	H	ND
1,N^6-etheno-cAMP	H	N1-C=C-N6	H	844 μM(1)
8-bromo-cAMP	H	NH_2	Br	724 μM(2)
8-amino-cAMP	H	NH_2	NH_2	ND
8-azido-cAMP	H	NH_2	N_3	103 μM(2)
8-methylamino-cAMP	H	NH_2	$NHCH_3^-$	356 μM(3)
8-benzylamino-cAMP	H	NH_2	$NHCH_5$	542 μM(1)
8-hydroxy-cAMP	H	NH_2	OH	841 μM(3)

[a] The chemical composition of C2, C6, and C8 positions are given, and the average values for $K_{0.5}$ for current activation are given with the number of measurements in parentheses. [b] No detectable binding.

however, Kaupp and colleagues (Eismann et al., 1993) have proposed a pentameric architecture similar to the structure of other ligand-gated channels.

cAMP, which differs from cGMP at the C2 and C6 positions (see Table 1), activated 39% of the maximal current in the patch shown in Figure 1. The $K_{0.5}$ for cAMP was 673 μM with an N_h of 1.7. We further explored the interaction between the C2 position and the binding pocket by exposing patches to N^2-monobutyryl-cGMP, which differs from cGMP by the addition of a relatively large butyryl substituent attached to the C2 amino nitrogen. The dose–response curve in Figure 1 was fitted with a $K_{0.5}$ of 313 μM and an N_h of 2.3. The normalized current is 61% of the cGMP-activated current in this patch.

It should be noted that the $K_{0.5}$ values determined from macroscopic currents are not binding constants but reflect contributions from both ligand binding and channel gating or activation. Each current measurement sums contributions

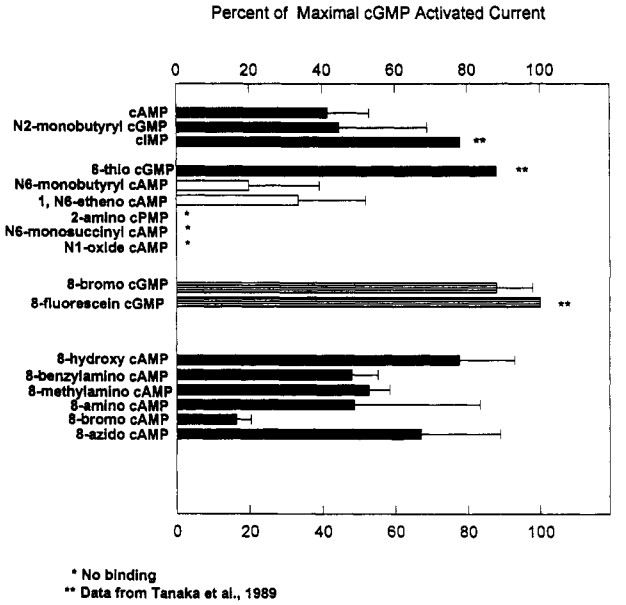

FIGURE 2: Averaged normalized current responses of cGMP analogues. Excised patches were perfused with 1 mM concentrations of the indicated analogue, and the current produced was normalized to that activated by 200 μM cGMP. Data from multiple patches were averaged, and the standard deviation of the mean is shown. The analogues are grouped according to the position on the purine rings which is altered; clear bars have alterations at C2, hatched bars have alterations at C6, and filled bars have alterations at the C8. Data for 6-thio-cAMP, cIMP, and 8-fluorescein-cGMP is taken from Tanaka et al. (1989). The $K_{0.5}$ values for cAMP and cGMP measured on frog rods were about twice those of salamander patches, indicating salamander channels are activated at lower concentrations. No differences were seen between these species in the fraction of current activated with cAMP, which was 37% (n = 7) in frog and 41% (n = 7) in salamander rods.

from hundreds or thousands of individual channels and reflects the channel conductance, the channel open time, and the probability of opening which is related to nucleotide binding. In the situation where only the binding affinity of the ligand is altered but not the conductance or kinetics of the channel opening and closing, we would expect the current to equal that activated by cGMP, and only the $K_{0.5}$ would be affected. In cases where the maximal current does not equal that of the cGMP response, changes in either the kinetics of the channel opening and closing or in channel conductance are implicated.

In Figure 2, average values of the current activated at 1 mM concentrations are shown for a number of cAMP and cGMP analogues. At this high concentration, the channel open probability is close to maximal since the ligand concentration is close to saturation. Changes in the maximal current at saturating concentrations probably reflect changes in the channel opening and closing kinetics in addition to changes in channel conductance. Analogues with alterations at C2 are shown with open bars at the top of the graph. Removal of the C2 amino group of cGMP produces cIMP, which activates 80% of the maximal current. The combined loss of the C2 amino and the replacement of the cGMP C6 keto with an amino group produces cAMP. This analogue activates 41% of the maximal current. In order to map analogue binding site contacts onto the channel function, the contacts must be considered within the context of all levels of protein structure. The functional probing of the binding

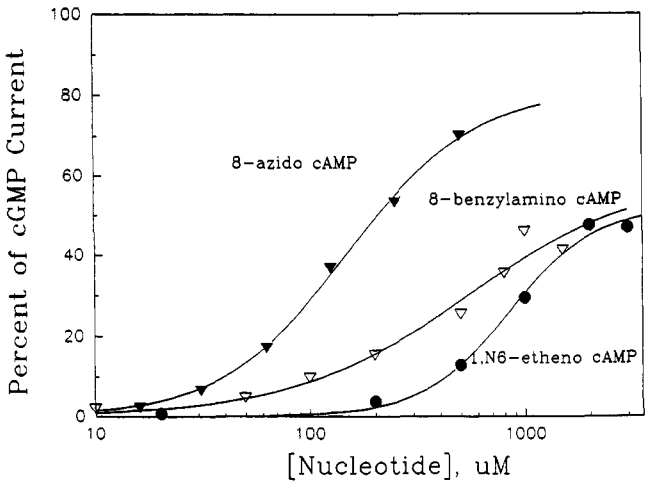

FIGURE 3: Normalized dose responses for 8-azido-cAMP, 8-benzylamino-cAMP, and 1,N^6-etheno-cAMP. Current responses were fitted as described above. The $K_{0.5}$ values for 8-azido-cAMP, 8-benzylamino-cAMP, and 1,N^6-etheno-cAMP were 150, 542, and 843 μM, respectively, with N_h values of 1.5, 1.0, and 2.1. The maximal currents were 81%, 60%, and 52%. Currents for 8-azido-cAMP and 1,N^6-etheno-cAMP were analyzed at +60 mV; others were +80 mV.

site with analogues will not lead to definitive correlations with ligand specificity or channel disposition, but when taken collectively, these data can help map general trends regarding interactions between the analogue and the binding site which translate to interactions between the binding site and other channel subdomains that may coordinate a particular channel property. An example of such interactions was shown in a recent study in which chimera forms of nucleotide-gated channel proteins were constructed from retinal and olfactory channels in order to examine structure–function properties (Goulding et al., 1994).

Table 1 summarizes the average $K_{0.5}$ values for a number of these analogues. The average for cGMP was 13.7 μM, and values for N^2-monobutyryl-cAMP and cAMP were 313 and 617 μM, respectively. The values for cGMP and cAMP for salamander patches are lower than those previously reported for frog rods [average $K_{0.5}$ values of 24 μM for cGMP and ~1.5 mM for cAMP (Tanaka et al., 1989)], suggesting that salamander channels may bind more tightly than frog channels. The relative selectivity for cGMP over cAMP is similar in these two species however and appears to be a general feature of retinal nucleotide-gated channels.

Alterations at the C6 and N1 Positions. Several analogues differing at C6 or N1 were examined in order to probe the interactions between the ligand and the binding pocket at these regions of contact. Figure 3 shows a normalized dose–response relation for 1,N^6-etheno-cAMP. N^6-Monobutyryl-cAMP was also active, although only 20% of the maximal current was activated in patches at 1 mM concentrations (data not shown). Attempts to determine the $K_{0.5}$ value for this derivative were unsuccessful however due to the small currents and our inability to saturate the response even at high concentrations.

In previous experiments, 2-amino-cPMP was shown not to activate the retinal channel (Tanaka et al., 1989). This analogue differs from cGMP by the loss of the C6 keto group, providing the first clues that contacts at C6 might be essential for binding in the retinal channel. Two additional analogues with alterations in the N1–C6 region, N^1-oxide-cAMP and N^6-monosuccinyl-cAMP, were tested in these experiments. Neither analogue activated any current in patches at 1 mM concentration. In order to determine whether the analogues might bind to the channel but fail to activate the conductance, each analogue was added in the presence of nonsaturating levels of cGMP. If the analogues bind, the current with the added analogue should be changed from that with cGMP alone [see data and discussion in Furman and Tanaka (1989)]. None of the inactive analogues affected the cGMP-activated currents, supporting the conclusion that they do not bind to the same cyclic nucleotide binding site as cGMP on the retinal channel.

The averaged currents activated for N^6-monobutyryl-cAMP and 1,N^6-etheno-cAMP at 1 mM are shown in Figure 2. Despite the addition of a ring between N1 and N6 in 1,N^6-etheno-cAMP, there is no significant change in either the maximal current or the $K_{0.5}$ values between the analogue and cAMP. With the exception of 6-thio-cGMP, previously examined (Tanaka et al., 1989), alterations at C6 decrease the maximal current by at least 2-fold and greatly diminish the apparent binding affinity.

Alterations at the C8 Position. A number of cAMP analogues with substituents at the C8 position were examined including 8-amino-, 8-azido-, 8-benzylamino-, 8-bromo-, 8-hydroxy-, and 8-methylamino-cAMP. Dose–response curves from 8-azido-cAMP and 8-benzylamino-cAMP are shown in Figure 3. Parameters from the fits are given in the figure legend, and average values for the current activation and $K_{0.5}$ are given for all analogues in Figure 2 and Table 1. The rank activity values for the cAMP series are 8-azido- > 8-methylamino- > 8-benzylamino- > cAMP > 8-bromo- > 8-hydroxy- ≫ 8-amino-cAMP. The comparison of currents at 1 mM concentrations shown in Figure 2 indicates that all C8 derivatives except 8-bromo-cAMP activate at least as much current as cAMP. 8-Hydroxyl-cAMP and 8-azido-cAMP produce considerably more current than cAMP. Also shown in Figure 2 are two cGMP analogues, 8-bromo-cGMP and 8-fluorescein-cGMP [taken from Tanaka et al. (1989)], both of which produce the maximal response in a patch.

One of the C8-substituted cAMP analogues was notably different from the others tested. 8-Amino-cAMP activated about 50% of the maximal current at 1 mM; however, attempts to determine the $K_{0.5}$ value were unsuccessful since the response could not be saturated even at high concentrations. This effect was seen on multiple patches and suggests that the amino substituent interacts with the binding site in a unique way.

Additional insights into C8 substituents may be derived by comparing these results with a series of cGMP analogues recently synthesized by Brown et al. (1993a). The experiments compared C8 substituents attached through either amino or thio linkages. The results showed that, regardless of the chemical nature of the terminal group, thio substitution at C8 produces more effective analogues than analogues coupled through an amino linkage. The $K_{0.5}$ values for thio-linked analogues were 20–80 times lower than the amino-linked analogues. Their results also showed that charge-neutral terminal groups form the most active derivatives. Negative groups decreased the activity somewhat while positively charged terminal residues were much less active. Earlier studies showed that C8 modifications in cGMP reduce $K_{0.5}$ values 10–50-fold for 8-bromo-cGMP (Brown et al.,

1993a; Zimmerman et al., 1985), 8-fluorescein-cGMP (Caretta et al., 1985; Tanaka et al., 1989), and 8-*p*-azidophenacylthio-cGMP (Brown et al., 1993b).

Our results on C8 substitutions on cAMP, taken with the results of Brown et al. (1993a) on cGMP analogues, suggest that neutral or hydrophobic groups decrease the $K_{0.5}$ of the ligand compared to that of the parent. In addition, the current activated by the C8-substituted cAMP analogues was greater than that produced by cAMP with the exception of 8-bromo-cAMP, suggesting that either the channel might be open longer or be more conductive due to contacts in the C8 region. Our results also support the conclusion by Brown et al. (1993a) that an amino group in the C8 position leads to an unfavorable interaction with the binding site.

In summary, the analogue studies indicate that the retinal rod channel binding site is tolerant of chemically and sterically diverse substituents even at points that contribute to the overall binding energy and the nucleotide specificity. All alterations at the C2 and C8 positions retain binding. The addition of nonpolar groups to C8 on cAMP actually increase the amount of current, suggesting that favorable interactions occur with the binding site through these substituents. Finally, alterations at C6 or N1 produce the only known inactive cyclic purine nucleotide analogues, suggesting that contacts in this region of the binding pocket are required for binding.

Molecular Modeling of the Ligand Binding Site Interaction

cGMP and cAMP are amphiphilic molecules with a polar ribofuranose moiety and a less polar purine moiety. Contacts to the retinal channel binding site from the polar ribofuranose moiety are essential for channel activation (Tanaka et al., 1989; Zimmerman et al., 1985). Contacts mediated by the purine moiety affect multiple channel functions, but the contacts mediating these functions are more tolerant of chemical alterations than the ribofuranose contacts. The relatively inflexible structure of the ring systems in cGMP analogues limits the conformational shifts during binding, and the analogues can therefore be used as steric probes of the binding site. The small size of the nucleotides also means that accurate molecular models can be computed, which will hopefully lead to a better understanding of the nucleotide binding domain. In the following section, we describe molecular models of the nucleotide analogues and the results of docking them into the model of the cGMP binding domain of the bovine retinal channel (Kumar & Weber, 1992). The correlation of nucleotide analogue electrophysiological data from salamander or frog rods with a structural model based on the bovine retinal channel is justified by the sequence conservation among the known retinal channels. To date, six retinal rod and cone channels have been cloned whose cDNA or mRNA encodes functional nucleotide-gated channels (Bonigk et al., 1993; Chen et al., 1993; Dhallan et al., 1992; Kaupp et al., 1989; Pittller et al., 1992). Within this family, all amino acid residues predicted to contact the nucleotide are conserved with the exception of one residue in the chick cone channel (Gly 605 in bovine rod is Asn 652 in chick cone).

Ligand Structures. Molecular models of active cyclic purine analogues are shown in similar orientations in Figure 4A. The top row shows cGMP, cAMP, and cIMP which differ chemically only at the C2 and C6 position. The next row shows the large, uncharged butyryl group attached at either N2 or N6. The butyryl substituents do not alter the conformation of the purine rings, but they may affect accessibility of the amino groups to hydrogen bonding. The C8 analogues shown include a small polar amino substituent and a large, hydrophobic benzylamino substituent. In general, the more rigid substituents and linkers are more useful as steric probes of the binding pocket because they undergo less conformational shift upon binding. In this regard, 1-N^6-etheno-cAMP is a good probe of the binding site at the C6 position because the extra ring should be quite rigid.

Figure 4B shows the inactive derivatives. N1 oxide is smaller than the etheno substituent; N^6-succinyl-cAMP has a large group attached with three carbon single bonds and a terminal-charged carboxyl residue. Also shown is 2-amino-cPMP, which is a C6 deoxy form of cGMP. Removal of the C6 oxygen on cGMP will change the electronic distribution in the rings since most of the cGMP is found in the keto form with the double bond of the ring shifted from the ring to the oxygen. The binding of cAMP, which should have an electron distribution in the six-membered purine ring similar to that of 2-amino-cPMP, suggests that the electronic nature of the ring alone does not determine binding and that contacts are required between the substituent at C6 and the binding site.

Predicted Analogue Contacts with the Binding Pocket. Our goal in building the analogue structures was to dock them into the model of the retinal channel binding domain in order to predict interactions between the analogues and the binding site. The proposed eight-stranded β-barrel secondary structure of the binding site model is shown in Figure 5A with N^2-monobutyryl-cGMP in the binding pocket. The first β-strand of the 8-stranded β-barrel is preceded by a short A helix, located some distance away from the nucleotide. Following the β8 strand, a short B helix is followed by a long C helix forming the remainder of the binding domain. The nucleotide is completely buried between the interior of the β-roll and the long C helix. Several hydrogen bonds are formed between the amino acid side chains of the β-sheets and the ribofuranose rings of the analogue. Several amino acids predicted to interact with the ligand are shown including Phe 533 on β5, Thr 560 on β7, Glu 544 between β6 and β7, and Ile 600 and Asp 604 on the C helix.

A closer view of N^2-monobutyryl-cGMP in the pocket is shown in Figure 5B with a selected group of amino acids. The region around the C2 position sterically accommodates this substituent with the butyryl group lying between Val 525 on β4 and Asn 562 on β7. Thr 560 is also shown, which was predicted by Kumar and Weber to form a hydrogen bond between the OH and the C2 amino group, thereby providing a structural basis for the cGMP selectivity of the retinal channel. The addition of the butyryl alters the position of the C2 amino group such that it can no longer form a hydrogen bond to the hydroxyl of Thr 560 consistent with the observed decrease in the $K_{0.5}$ for the N^2-monobutyryl-substituent.

Contacts at the C6 position are illustrated by the model of 1,N^6-etheno-cAMP in the binding pocket shown in Figure 5C. The modeling shows that the etheno ring can be sterically accommodated. This projection was selected to emphasize the relative orientation of the etheno ring to the

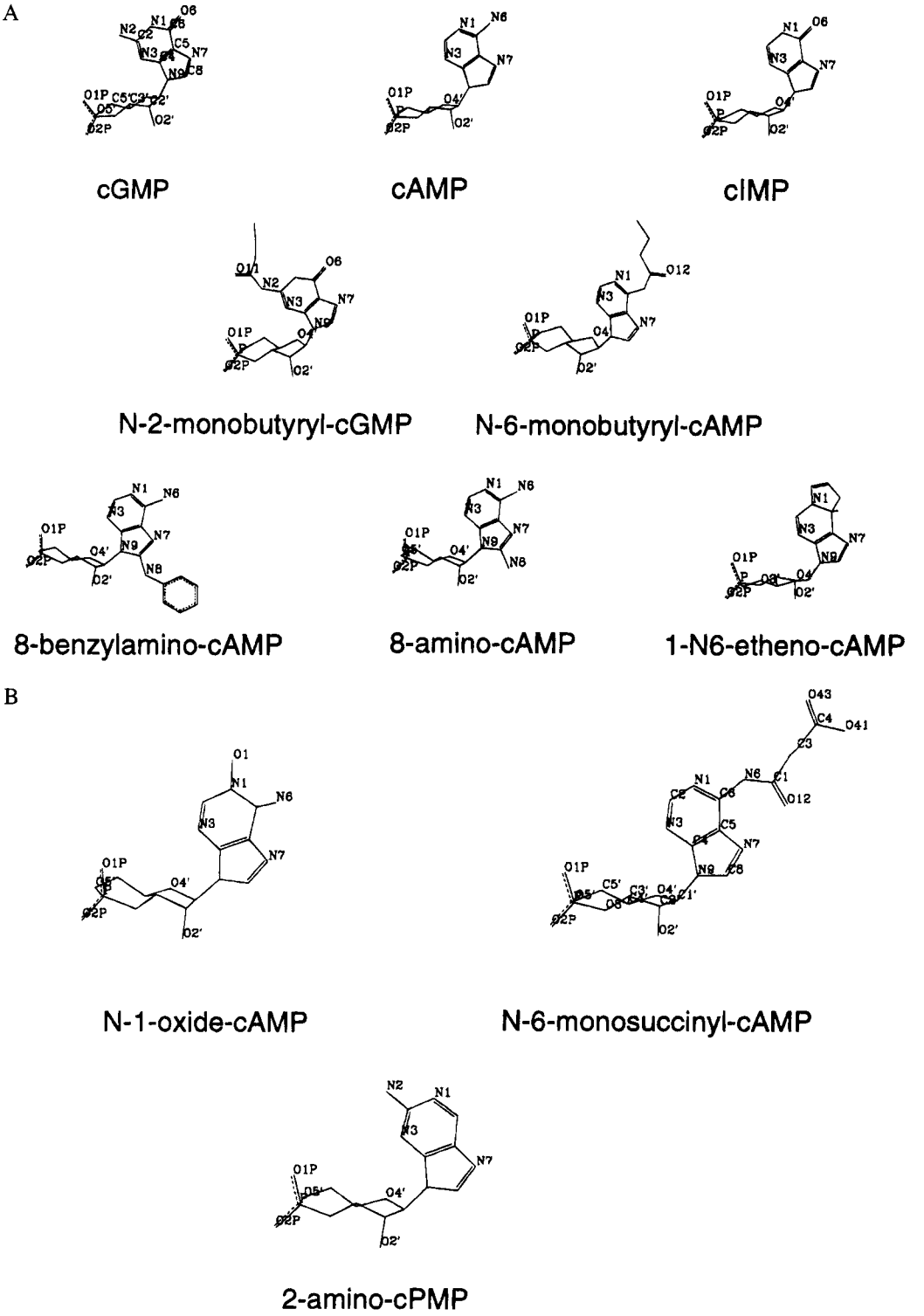

FIGURE 4: Molecular models of active cyclic nucleotide derivatives (A) and inactive derivatives (B). Molecular models of the nucleotide derivatives were constructed using the molecular modeling tools in InsightII as described in the Methods. The inactive derivatives all have alterations at the C6 position.

purine rings and to Phe 533 on β5. Simultaneous additions to the N1 and C6 positions on 1-N^6-etheno-cAMP force these atoms into sp^3 orbital configurations with bond angles of 109° as opposed to the sp^2 orbital 120° angles. This addition results in a pucker in the six-membered purine ring that can be seen at the edge of the ring in Figure 5C.

The presence of a derivative in the C6 position on the nucleotide affects the position of the phenyl group of Phe 533 in the pocket. This is shown in Table 2 by the > 160° Phe 533 side chain dihedral angle for cGMP, cAMP, and 1,N^6-etheno-cAMP. The dihedral angle for 2-amino-cPMP, which does not activate the channel, is less than 160°. The negative polar keto group of cGMP draws the phenyl edge toward the purine as indicated by the 133° phenyl dihedral angle. The positive polar amino group of cAMP causes the phenyl ring to realign facing the purine as indicated by the 30° increase in the dihedral angle. The phenyl dihedral angle for 1,N^6-etheno-cAMP falls between cGMP and cAMP, reflecting the nonpolar nature of the etheno substituent. Since the nearest amino acids to the C6 position in the binding

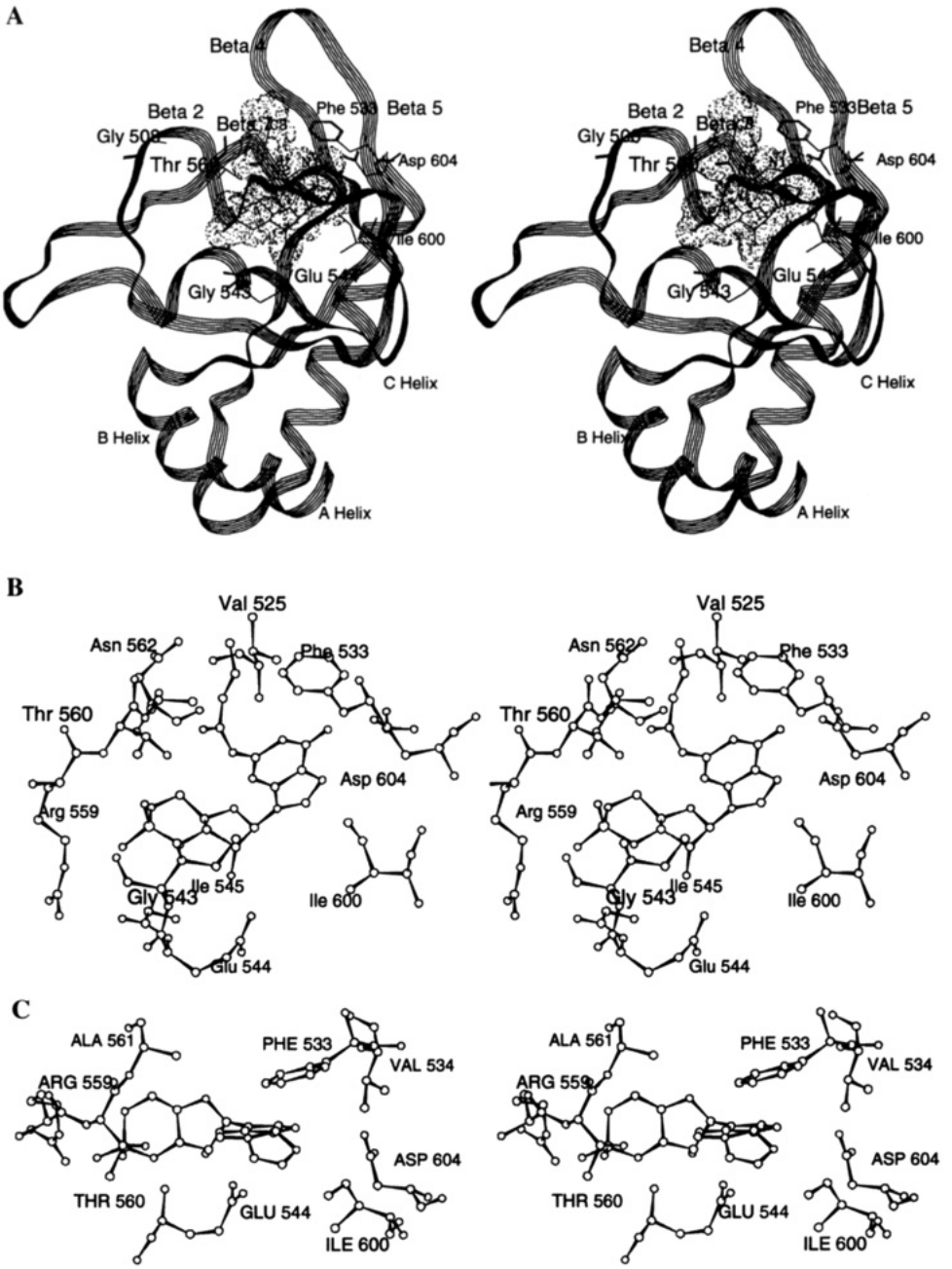

FIGURE 5: (A) Stereo view of N^2-monobutyryl-cGMP in the retinal channel binding pocket. The binding site was derived from the coordinates of the retinal binding site model with the ligand placed in the pocket and minimized as described in the Methods. The secondary structure of the binding domain, spanning residues 485−609, was assigned by Kumar and Weber (1992) as indicated. Several residues predicted to contact the ligand are also shown including Thr 560 and Glu 544, which are predicted to form hydrogen bonds with the ribofuranose rings. (B) Predicted contacts between N^2-monobutyryl-cGMP and the binding site. A stereo view of N^2-monobutyryl-cGMP in the binding pocket with selected residues in a 5-Å radius of the ligand. The predicted hydrogen bond between the N^2-amino group and the OH on Thr 560 is disrupted by the presence of the butyryl substituent. This view shows that the binding site sterically accommodates the substituent. (C) Predicted contacts between 1,N^6-etheno-cAMP and the binding site. The orientation of the ligand in the binding site has been adjusted to show the interaction with Phe 533.

site model are Phe 533 and Asp 604, the Phe side chain might interact in a weakly electrostatic donor−acceptor manner with the C6 substituent contributing significantly to the total binding energy (Levitt & Perutz, 1988). Although benzene rings are considered nonpolar, the π electrons in the aromatic Phe ring are localized above and below the face of the ring, giving a partial negative charge to the face and a partial positive charge to the hydrogens at the edge of the ring. The electronegative oxygen in cGMP and the sulfur atom in 6-thio-cGMP might interact favorably with the edge of the ring while the C6 amino group in cAMP might share its partial positive charge with the ring face. The results in Table 2 support the idea that the side chain of Phe 533 shifts its orientation in response to changes in the C6 substituent.

Figure 6A shows 8-benzylamino-cAMP in the pocket, illustrating the steric accommodation of the C8 substituents between the C helix and β5. This model is representative of the accommodation of all C8 analogues. A close up view of 8-amino-cAMP is shown in Figure 6B. Note the hydrophobic amino acids closest to the C8 amino groups including Ile 600, Val 534, and Leu 536 and the basic Lys 596. The location of the polar C8 amino near to the lysine in the midst of three hydrophobic residues might account for the loss of activity seen with C8 amino substitutions.

Table 2: Dihedral Angles Predicting Phe 533 Orientation[a]

nucleotide	side chain tilt C-Cα-Cβ-Cγ	phenyl tilt Cα-Cβ-Cγ-Cδ
cGMP	162	133
cAMP	164	162
N^6-etheno-cAMP	163	155
2-amino-cPMP[b]	155	131

[a] The nucleotides were minimized in the binding site as described in the Methods. The C-Cα-Cβ-Cγ angle refers to the dihedral angle between the amino acid backbone represented by C (carboxyl carbon) and Cα (alpha carbon) and tilt of the side chain Cβ (β carbon) to Cγ (first carbon in the benzyl ring). The phenyl side chain tilt is shown by dihedral angle Cα and Cβ to Cγ and Cδ (both in the phenyl ring). [b] Does not bind to the cGMP binding site as shown by competition studies (Tanaka et al., 1989).

For comparison, we examined the location of 8-hydroxyl-cAMP (not shown). This analogue produces more current than either 8-amino-cAMP or cAMP, but the $K_{0.5}$ is nearly equal to that of cAMP. In this case, the modeling predicts that the C8 polar hydroxyl substituent is capable of forming hydrogen bonds with Lys 596 and Glu 544, possibly accounting for the more favorable interaction of the hydroxyl at C8.

A limitation of the modeling was apparent with 8-fluorescein-cGMP. Using the energy minimization procedures described in the Methods, we were unable to dock this highly active analogue in the binding site without steric collisions. The analogue has a fluorescein group linked to C8 guanine through a thiomethylcarbamoyl linkage (Caretta et al., 1985); the four single bonds of the linker introduce flexibility to the substituent, but the terminal rings of fluorescein are planar and rigid. Many conformations of this analogue are likely present in solution; particular conformations induced by binding are not easily predicted by molecular modeling.

One final point about the modeling relates to the most active cAMP analogue, 8-azido-cAMP. InsightII had no force field parameters for constructing the azido group; therefore, two alternative approaches were employed. The first was to construct the terminal group of 8-azido-cAMP using carbon with two double bonds in place of nitrogens in order to approximate the steric constraints of fitting the derivative in the pocket. Following minimization of the entire model structure, nitrogens replaced the carbons in order to observe possible interactions and labeling sites. Since photoactivation of the azido cleaves the two terminal nitrogens, resulting in a single reactive nitrogen, the second approach was to use the 8-amino-cAMP analogue to determine possible cross-linking sites. As shown by the 8-amino-cAMP analogue in Figure 6B, there are no close residues in this region for covalent bonding to occur between the reactive nitrogen and the binding site. This prediction is consistent with the report that 8-azido-cGMP does not photolabel the retinal channel (Thompson & Khorana, 1990).

In several cAMP analogues, additional hydrogen bonds were predicted between the purine and the binding site. Most of these involved contacts between the N6 and Asp 604 on

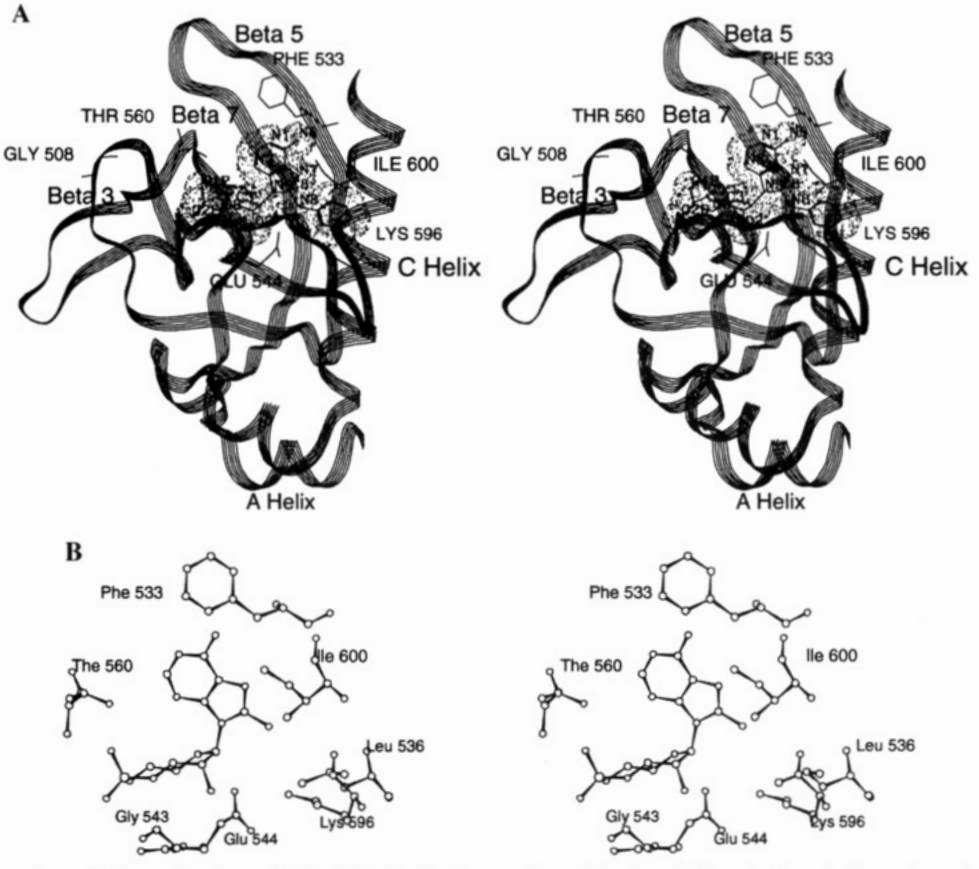

FIGURE 6: (A) Stereo view of 8-benzylamino-cAMP within the binding pocket. The phenyl ring of this substituent is sterically accommodated in the binding pocket of the binding site model lying close to the C helix. (B) Predicted contacts between 8-amino-cAMP and the binding site. A stereo view shows 8-amino-cAMP is located in the midst of several hydrophobic amino acids and Lys 596. The closest distances between the C8 amino and the residues are 4.96 Å to Glu 544, 4.5 Å to Ile 600, 4.8 Å to Leu 586, 4.08 Å to Leu 536, and 4.11 Å to Lys 596. In contrast, the hydroxyl group of 8-hydroxyl-cAMP is positioned 2.82 Å from Lys 596, 2.87 Å from Glu 544, 5.74 Å from Val, and 5.85 Å from Ile 600.

the C helix. The existence and position of the C helix in the retinal binding site could not be well-established by the CAP crystal structure due to large sequence differences in this region, resulting in uncertainty about these predictions (Kumar & Weber, 1992). Independent direct evidence of the importance of the putative C-helical region in nucleotide binding was recently obtained from olfactory and retinal channel chimeras (Goulding et al., 1994).

DISCUSSION

The experimentally determined structure of CAP with cAMP bound shows cAMP is bound in the anti conformation. cGMP-dependent kinase was modeled with cGMP in the syn conformation (Weber et al., 1989) as was the retinal binding site (Kumar & Weber, 1992). Mutagenesis experiments involving Thr 560 on β7 of the retinal channel (Altenhofen et al., 1991) as well as mutations of the equivalent residue on the cyclic nucleotide-dependent kinases (Shabb et al., 1990, 1991) support the syn conformation for cGMP since amino acids such as alanine, which cannot form hydrogen bonds with the C2 amino group, result in a significant loss of apparent binding energy for cGMP. Our modeling was initiated with all analogues in the syn position, based on the coordinates from the original model (Kumar & Weber, 1992), and the conformation of the nucleotides did not change as the bound ligands were energy minimized. Since no hydrogen bonds are predicted to occur between the purine rings of cAMP and the retinal channel binding site, models of cAMP in the anti conformation were also minimized in the retinal binding site. Results with the anti conformation of several analogues showed cGMP, cAMP, 8-aminobenzyl-cAMP, and N^2-monobutyryl-cGMP were sterically accommodated in the binding site. For cGMP, no hydrogen bonds were predicted from the purine of the anti conformation to the binding site since the C2 position is rotated away from Thr 560. The predicted interactions between Phe 533 and the purine C6 substituent of the syn conformations of both cAMP and cGMP are also lost due to reduced packing of the hydrophobic residues in the region including Phe 533. Modeling of the anti conformation of 8-aminobenzyl-cAMP places the benzyl C8 substituent outside the binding domain. Such an interaction between a benzyl substituent and water would be energetically costly and would not be consistent with the electrophysiological data showing that the analogue has a lower $K_{0.5}$ than cAMP. The conformation of the ligands in the binding site will require experimental study of the actual structure of the bound ligand in the channel.

The cGMP preference demonstrated by all known retinal channels and cGMP-dependent kinases is thought to be mediated through a hydrogen bond from Thr 560 (retinal channel) on β7 to the C2 amino group on guanine, and a number of site-specific mutation studies support this idea (Shabb et al., 1991, 1990; Altenhofen et al., 1991). This hydrogen bond is not required for binding or channel activation however, as shown by cAMP activation of the current in excised retinal patches. In addition to retinal channels, the sequences of a number of closely related nucleotide-activated channels from olfactory neurons are also known [reviewed by Zufall et al. (1994)], and all these channels conserve the threonine residue. Interestingly, nucleotide-activated currents in most olfactory neurons show little discrimination between cGMP and cAMP (Zufall et al., 1994; Frings et al., 1992). In rat, a second nucleotide-gated olfactory channel subunit was recently cloned (Liman & Buck, 1994). Channels expressed from rOCNC1 show a ~30-fold preference for cGMP (Dhallan et al., 1990). The rOCNC2 subunit (Liman & Buck, 1994) does not express alone, but when both subunits are co-expressed in oocytes, the cGMP preference is reduced to ~3-fold. It would appear from these experiments, as well as from a number of observations on retinal channels [for a review, see Koutalos and Yau (1993)], that post-translational modifications and cellular regulation, including heterogeneous subunit assembly, modulate cyclic nucleotide-gated channel properties in sensory cells. Our recent molecular modeling of olfactory channel binding sites suggests unique strategic interactions between the binding site and cAMP, which may replace part of the energy loss due to the absence of the hydrogen bond between Thr 560 and the N2 amino group of cGMP (Scott et al., 1995).

One important distinction between the structure of CAP and the retinal binding site models should be noted. In CAP, the C6 amino group of cAMP forms hydrogen bonds with Thr 127 on the C helix of one subunit of the dimer and also to Ser 128 of the C helix of the other subunit (Weber & Steitz, 1987). The finding that cGMP and cIMP also bind to CAP but do not initiate DNA binding suggests that cAMP-mediated intersubunit contacts are essential for activation of CAP. The bovine retinal channel model is limited to a single subunit binding site, although the channel is multimeric with cooperative activation of the current. It is possible that intersubunit contacts similar to those in CAP are involved in the cooperative activation of cyclic nucleotide-activated channels.

In conclusion, we offer a highly speculative scheme for ligand binding based on analogue studies and molecular modeling. Both the CAP structure and the retinal binding site model show the nucleotide buried within the channel binding site, implying that the binding site 'opens' to permit diffusion of the ligand to and from the cytosol. As the nucleotide enters the binding site, the side chains of Asp 604, Glu 544, and Arg 559 could provide guidance to seat the nucleotide. This initial contact might induce the pocket to fold around the nucleotide drawing Phe 533 toward the purine. How could Asp 604 guide both cGMP and cAMP when cGMP is being repulsed by the carboxyl group of the aspartic acid side chain? In the case of cGMP, cIMP, and 6-thio-cGMP, a water might be recruited to hydrogen bond between the Asp 604 and the incoming nucleotide. As the Phe 533 moves into position, the water would be expelled, and Asp 604 would move away from the C6 keto group on cGMP. For cAMP and the cAMP analogues, the C6 amino group might interact favorably with the side chain of Asp 604. Several experimental observations are consistent with this type of mechanism. First, the lack of binding of 2-amino-cPMP could be explained by the absence of a C6 substituent that is needed to position the β5 and/or the C helix. Also the carboxyl group of the N^6-monosuccinyl-cAMP might repulse the Asp 604, preventing the alignment of the C helix. Finally, the inability of N^1-oxide-cAMP to bind to the channel may be due to the simultaneous presence of a negative and positive polar substituent in the N1−C6 region of the purine disrupting the required alignment of Phe 533.

ACKNOWLEDGMENT

We thank Drs. Jannette Carey, Jim Lear, Irene Weber, and Gregg Wells for their careful reading of the manuscript and for useful discussions of the work.

REFERENCES

Altenhofen, W., Ludwig, J., Eismann, E. W., Bonigk, W., & Kaupp, U. B. (1991) *Proc. Natl. Acad. Sci. U.S.A. 88*, 9868.

Bonigk, W., Altenhofen, W., Muller, J., Dose, A., Illing, M., Molday, R. S., & Kaupp, U. B. (1993) *Neuron 10*, 865.

Brown, R., Bert, R., Evans, F., & Karpen, J. (1993a) *Biochemistry 32*, 10089.

Brown, R., Gerber, W., & Karpen, J. (1993b) *Proc. Natl. Acad. Sci. U.S.A. 90*, 5369.

Caretta, A., Cavaggioni, A., & Sorbi, R. T. (1985) *Eur. J. Biochem. 153*, 49.

Chen, T. Y., Peng, T. W., Dhallan, R. S., Ahamed, B., Reed, R. R., & Yau, K. W. (1993) *Nature 362*, 764.

Dhallan, R. S., Yau, K., Schrader, K. A., & Reed, R. R. (1990) *Nature 347*, 184.

Dhallan, R. S., Macke, J. P., Eddy, R. L., Shows, T. B., & Reed, R. R. (1992) *J. Neurosci. 12*, 3248.

Druyan, M. E., Sparagana, M., & Peterson, S. W. (1976) *J. Cyclic Nucleotide Res. 2*, 373.

Eismann, E., Bonigk, W., & Kaupp, U. B. (1993) *Cell Physiol. Biochem. 3*, 332.

Frings, S., Lynch, J. W., & Lindemann, B. (1992) *J. Gen. Physiol. 100*, 45.

Furman, R. E., & Tanaka, J. C. (1989) *Biochemistry 28*, 2784.

Furman, R. E., & Tanaka, J. C. (1990) *J. Gen. Physiol. 96*, 57.

Goulding, E. H., Tibbs, G. R., & Seigelbaum, S. A. (1994) *Nature 372*, 369.

Hille, B. (1992) *Ionic Channels of Excitable Membranes*, pp 236–258, Sinauer Associates, Inc., Sunderland, MA.

Kaupp, U. B. (1991) *Trends Neurosci. 14*, 150.

Kaupp, U. B., Niidome, T., Tanabe, T., Terada, S., Bonigk, W., Stuhmer, W., Cook, N. J., Kangawa, K., Matsuo, H., Hirose, T., Miyata, T., & Numa, S. (1989) *Nature 342*, 762.

Koutalos, Y., & Yau, K. (1993) *Curr. Opin. Neurobiol. 3*, 513.

Kumar, V. D., & Weber, I. T. (1992) *Biochemistry 31*, 4643.

Levitt, M. & Perutz, M. (1988) *J. Mol. Biol. 201*, 751.

Liman, E. R., & Buck, L. B. (1994) *Neuron 13*, 611.

MacKinnon, R. (1991) *Nature 350*, 232.

McKay, D. B., Weber, I. T., & Steitz, T. A. (1982) *J. Biol. Chem. 257*, 9518.

Pittller, S. J., Lee, A. K., Altherr, M. R., Howard, T. A., Seldin, M. F., Hurwitz, R. L., Wasmuth, J. J., & Baehr, W. (1992) *J. Biol. Chem. 267*, 6257.

Scott, S.-P., Epstein, A. J., Lopez, M. C., & Tanaka, J. C. (1994) *Biophys. J. 66*, A437.

Scott, S.-P., Harrison, R. W., Weber, I. T., & Tanaka, J. C. (1995) *Biophys. J. 68*, A147.

Shabb, J. B., Ng, L., & Corbin, J. D. (1990) *J. Biol. Chem. 265*, 16031.

Shabb, J. B., Buzzeo, B. D., Ng, L., & Corbin, J. D. (1991) *J. Biol. Chem. 266*, 24320.

Weber, I. T., & Steitz, T. A. (1987) *J. Mol. Biol. 198*, 311.

Yau, K.-W., & Baylor, D. A. (1989) *Annu. Rev. Neurosci. 12*, 289.

Zimmerman, A. L., Yamanaka, G., Eckstein, F., Baylor, D. A., & Stryer, L. (1985) *Proc. Natl. Acad. Sci. U.S.A. 82*, 8813.

Zufall, F., Firestein, S., & Shepherd, G. M. (1994) *Annu. Rev. Biophys. Biomol. Struct. 23*, 577.

BI942021+